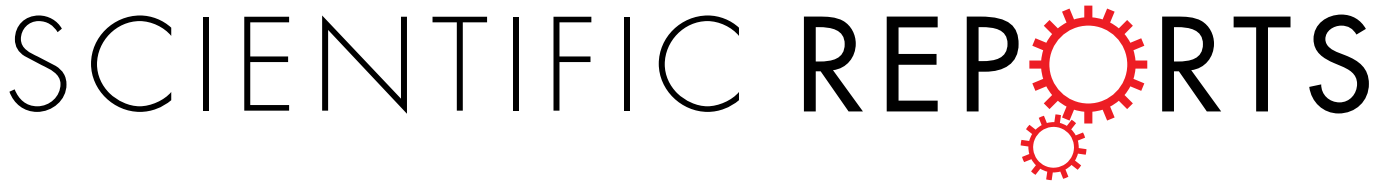

OPEN

Blue-green tunable color of Ce^{3+}/Tb^{3+} coactivated $NaBa_3La_3Si_6O_{20}$ phosphor via energy transfer

Received: 29 April 2016
Accepted: 24 August 2016
Published: 15 September 2016

Zhen Jia[1,2,3] & Mingjun Xia[2]

A series of color tunable phosphors $NaBa_3La_3Si_6O_{20}:Ce^{3+}$, Tb^{3+} were synthesized via the high-temperature solid-state method. $NaBa_3La_3Si_6O_{20}$ crystallizes in noncentrosymmetric space group *Ama2* with the cell parameters of a = 14.9226(4) Å, b = 24.5215(5) Å and c = 5.6241(2) Å by the Rietveld refinement method. The Ce^{3+} ions doped $NaBa_3La_3Si_6O_{20}$ phosphors have a strong absorption band from 260 to 360 nm and show near ultraviolet emission light centered at 378 nm. The Ce^{3+} and Tb^{3+} ions coactivated phosphors exhibit color tunable emission light from deep blue to green by adjusting the concentration of the Tb^{3+} ions. An energy transfer of $Ce^{3+} \rightarrow Tb^{3+}$ investigated by the photoluminescence properties and lifetime decay, is demonstrated to be dipole–quadrupole interaction. These results indicate the $NaBa_3La_3Si_6O_{20}:Ce^{3+}$, Tb^{3+} phosphors can be considered as potential candidates for blue-green components for white light emitting diodes.

By virtue of the special merits of high brightness, energy-efficient, life-durable, and environmentally friendly, the white light emitting diodes (w-LEDs) made from blue or near-ultraviolet (*n*-UV) emitting LEDs chips coated with phosphors have the potential to overtake incandescent and fluorescent lighting types[1–4]. In 1996, the w-LEDs fabricated from the blue-emitting InGaN LED chips combined with the yellow-emitting phosphors (YAG:Ce^{3+}) were commercialized[5]. Unfortunately, this technology has the following problems: low color rendering index due to two-color mixing, and low color reproducibility due to the strong dependence of white color purity on the quality of phosphors[6–11]. To solve these problems, the w-LEDs had been fabricated employing blue, green and red emitting phosphors excited by a blue or *n*-UV chip[12–14]. However, the strong reabsorption of blue light by red and green phosphors reduces the luminescence efficiency in this system[15,16]. To overcome these disadvantages, vigorous attentions were received to exploit the emission-tunable phosphors with strong absorption in *n*-UV region[17,18]. Simultaneously, an energy transfer can obviously improve the luminescent efficiency and color reproducibility as well as widen the emission spectra of phosphors.

After years of efforts, a series of promising phosphors had been developed, such as fluorides[19], silicates[20,21], phosphates[12], orthovanadates[22,23], borates[24,25], tungstates/molybdates[26,27], nitrides[28,29], aluminates[30–32], etc. Among them, the silicate compounds as luminescent hosts were intensively studied because of their remarkable stability of physical and chemical properties, flexible crystal structures and relatively easy preparation process. Among rare earth ions, the Tb^{3+} ion is the best candidate for green component due to its predominant $^5D_4$–$^7F_5$ transitions peaking at around 545 nm[33]. However, the electric dipole transitions within the 4*f* configurations of the Tb^{3+} ion is spin forbidden, resulting in the weak intensity of its absorption in the *n*-UV region and the narrow width. Thus, a suitable sensitizer is always necessary for the phosphors activated by the Tb^{3+} ion. It is well known that the Ce^{3+} ion is an excellent sensitizer transferring a part of its energy to an activator such as the Tb^{3+} ion depending on its lowest 5d state and broad absorption and emission bands from the allowed $4f \rightarrow 5d$ transitions[34]. In this work, we reported a novel silicate host phosphor, $NaBa_3La_3Si_6O_{20}:Ce^{3+}$, Tb^{3+} for the excitation by a *n*-UV LED chip, and the crystal structure, luminescent properties and energy transfer mechanism between the Ce^{3+} ion and the Tb^{3+} ion had been thoroughly investigated.

[1]Key Laboratory of Coordination Chemistry and Functional Materials in Universities of Shandong, Dezhou University, Dezhou 253023, PR China. [2]Beijing Center for Crystal Research and Development, Key Laboratory of Functional Crystals and Laser Technology, Technical Institute of Physics and Chemistry, Chinese Academy of Sciences, Beijing 100190, PR China. [3]University of Chinese Academy of Sciences, Beijing 100049, PR China. Correspondence and requests for materials should be addressed to M.X. (email: xiamingjun@mail.ipc.ac.cn)

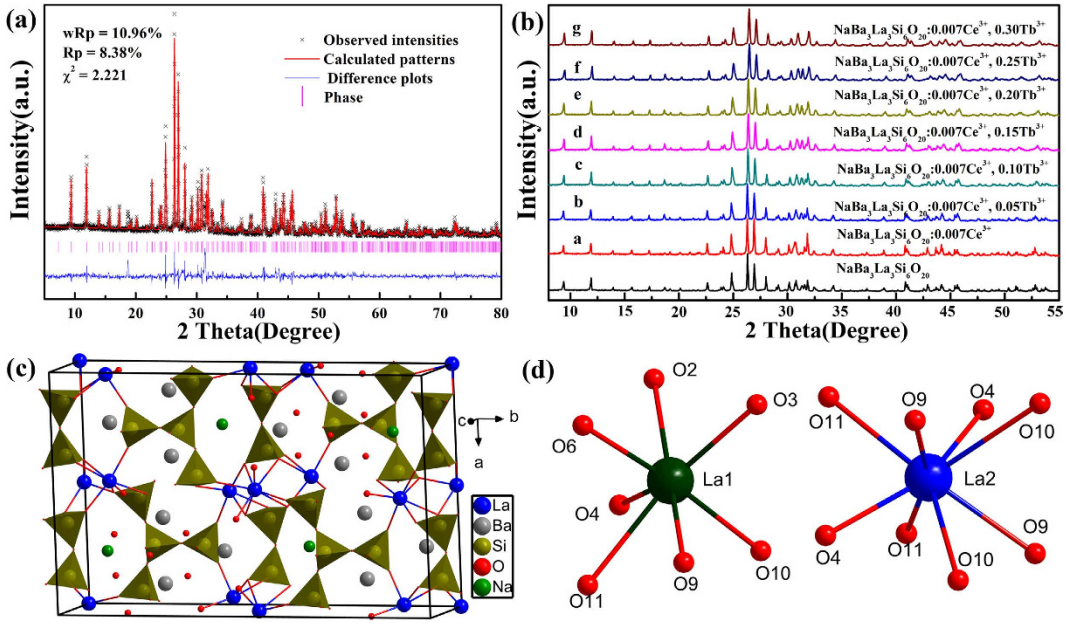

Figure 1. (**a**) The XRD profiles for the Rietveld refinement of $NaBa_3La_3Si_6O_{20}$. (**b**) The XRD patterns of the $NaBa_3La_3Si_6O_{20}$, $NaBa_3La_3Si_6O_{20}$:0.007Ce^{3+} and $NaBa_3La_3Si_6O_{20}$:0.007Ce^{3+}, yTb^{3+} phosphors. (**c**) The structure of unit cell of $NaBa_3La_3Si_6O_{20}$ along the c axis. (**d**) The coordination environments of La1 and La2 in $NaBa_3La_3Si_6O_{20}$.

Results and Discussion

Crystal structure and phase formation. Figure 1(a) demonstrates the observed and calculated XRD patterns as well as their difference for the Rietveld refinement of $NaBa_3La_3Si_6O_{20}$. In the refinement, an initial structure model and atomic positions of $NaBa_3Eu_3Si_6O_{20}$ were adopted for the structure refinement[35,36]. $NaBa_3La_3Si_6O_{20}$ crystallizes in the noncentrosymmetric space group *A*ma2 and unit cell parameters are obtained as a = 14.9226(4) Å, b = 24.5215(5) Å and c = 5.6241(2) Å, which are slightly larger than those of $NaBa_3Eu_3Si_6O_{20}$ due to large ionic radius of La^{3+} ion[37]. As shown in Fig. 1(c), the basic structural units are distorted $(SiO_4)^{4-}$ tetrahedra which are further linked by the Ba, La, and Na atoms to build a complex three-dimensional framework. The Na atoms which are surrounded by six oxygen adopt distorted pentagonal-pyramidal geometry, the Ba1 and Ba2 atoms coordinated to seven and eight oxygen are in distorted trigonal prism and cube configuration. In the structure of $NaBa_3La_3Si_6O_{20}$, there are two kinds of La sites, implying that there are two possible types of Ce^{3+} ions in the $NaBa_3La_3Si_6O_{20}$:Ce^{3+} samples. The La1 atoms are coordinated to seven oxygen atoms to form pentagonal bipyramid while the La2 surrounded by eight oxygen atoms are in square anti-prism environment (Fig. 1(d)).

Figure 1(b) shows the selected XRD patterns of the as-synthesized representative samples of $NaBa_3La_3Si_6O_{20}$ and $NaBa_3La_3Si_6O_{20}$:0.007Ce^{3+}, yTb^{3+} ($0 \le y \le 0.30$) and the quantitative analysis of all the samples illustrate that the doping of Ce^{3+} or/and Tb^{3+} are successful (Supplementary Table S1). Also, it can be seen that all the diffraction peaks of the selected phosphors match well with the $NaBa_3La_3Si_6O_{20}$ phase. Even at high doping concentration of the Tb^{3+} ion (30%), the XRD patterns of phosphors are almost same with that of undoped phase, which illustrates the excellent stability and accommodation capacity for doped ions of crystal structure of the $NaBa_3La_3Si_6O_{20}$ host. The XRD profiles for the Rietveld refinement of the single element doped and co-doped samples and the coordination, occupancy and isotropic displacement parameter for all samples are listed (Supplementary Figs S1–S7, Tables S2–S9).

Photoluminescence properties and energy transfer. As shown in Fig. 2(a), the PLE spectra of the $NaBa_3La_3Si_6O_{20}$:0.007Ce^{3+} sample consist of three absorption bands centered at around 254, 282 and 331 nm, which arise from the electronic transitions between the ground state ($^2F_{5/2}$ and $^2F_{7/2}$) and the levels of 5*d* excited split by crystal field of the Ce^{3+} ion[38]. Under the excitation wavelength of 331 nm, the Ce^{3+} ion doped $NaBa_3La_3Si_6O_{20}$ sample shows an asymmetric emission band extending from 340 to 500 nm with the maximum at 378 nm, indicating a possible spectral overlap originating from different luminescence centers. It is obvious that one type of Ce^{3+} ions gives rise to two emission band due to the transitions from the lowest 5*d* excited states to two ground states ($^2F_{7/2}$ and $^2F_{5/2}$) respectively[39]. However, the emission band of the $NaBa_3La_3Si_6O_{20}$:0.007Ce^{3+} sample can be decomposed into four Gaussian components A–D peaking at 364, 380, 394 and 410 nm with the energy gaps between A and C is 2092 cm^{-1}, that of B and D is 1926 cm^{-1}, which are close to the theoretical value of 2000 cm^{-1} [40,41]. These results imply that there should be two kinds of Ce^{3+} ions, which is consistent with the previous investigation on the crystal structure that there are two kinds of different chemical environment of La^{3+} ions in the $NaBa_3La_3Si_6O_{20}$ host.

As given in Fig. 2(b), the PL intensity of the $NaBa_3La_3Si_6O_{20}$:xCe^{3+} samples increases gradually with the increase of the doping concentration of the Ce^{3+} ions and reaches the maximum when the *x* value is 0.007,

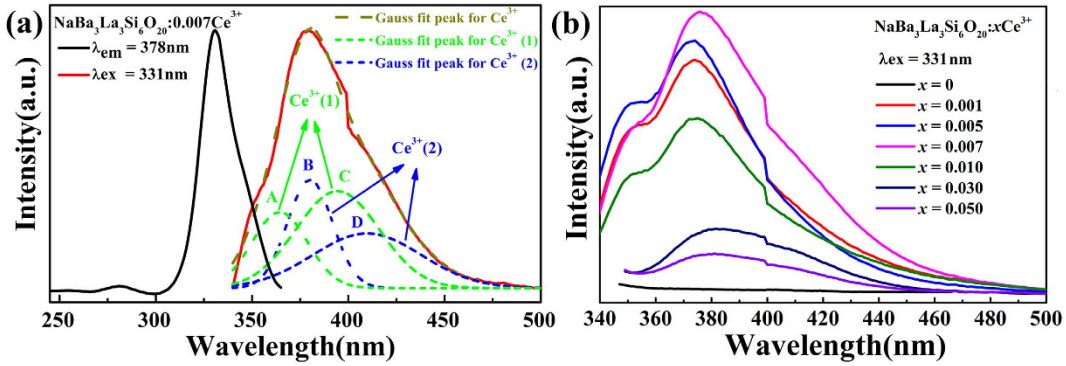

Figure 2. (**a**) The PLE (dark solid line) and PL spectra (red solid line) of the $NaBa_3La_3Si_6O_{20}$:0.007Ce^{3+} sample and the Gaussian peaks fitting (the green dashed lines of the Ce^{3+} (1) and the blue dashed lines of the Ce^{3+} (2)). (**b**) The PL spectra of the $NaBa_3La_3Si_6O_{20}$:$x$$Ce^{3+}$ samples with varying concentration of the Ce^{3+} ions.

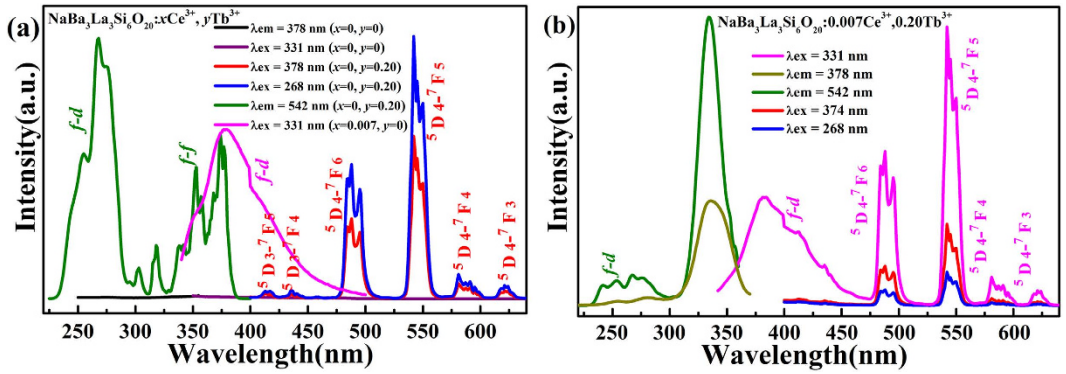

Figure 3. The PLE and PL spectra of the $NaBa_3La_3Si_6O_{20}$:$x$$Ce^{3+}$, $y$$Tb^{3+}$ phosphors (**a**), and the $NaBa_3La_3Si_6O_{20}$: 0.007Ce^{3+}, 0.20Tb^{3+} phosphor (**b**).

and then begins to decrease due to concentration quenching[42]. It is also indicated that the Ce^{3+} ion is a sensitizer for the Tb^{3+} ion and an energy transfer of $Ce^{3+} \rightarrow Tb^{3+}$ is crucial to enhance green emission of the Tb^{3+} ion and achieve color tunable emission light. Therefore, the optimal concentration of the Ce^{3+} ion in the $NaBa_3La_3Si_6O_{20}$:$x$$Ce^{3+}$ samples is confirmed to be 0.007.

Generally, the critical distance R_C between the Ce^{3+} ions can be calculated with the following equation given by Blasse[43]:

$$Rc = 2\left[\frac{3V}{4\pi xN}\right]^{1/3} \quad (1)$$

where V is the volume of unit cell, x is the critical concentration of doped ions, where the emission intensity of phosphors reaches the maximum, N is the number of host cations per unit cell. For the $NaBa_3La_3Si_6O_{20}$:0.007Ce^{3+} sample, $N = 12$, $V = 2057.989$ Å^3, R_C is calculated to be about 25.00 Å. Dexter noted a non-radiative energy transfer usually was attributed to exchange or multipole – multipole interaction in oxide phosphors and the exchange interaction was valid only when the Rc was shorter than 5 Å[44]. In consequence, the concentration quenching mechanism of the Ce^{3+} ions in the $NaBa_3La_3Si_6O_{20}$:$x$$Ce^{3+}$ samples is dominated by the multipole – multipole interaction.

Figure 3(a) depicts the PLE and PL spectra of the $NaBa_3La_3Si_6O_{20}$:0.20Tb^{3+} sample. The PLE spectrum monitored at 542 nm exhibits a broad absorption band centered at 268 nm from 200 to 300 nm and several peaks within the scope of 300 to 400 nm. The former excited peak is ascribed to $4f^8$–$4f^7 5d$ transition of the Tb^{3+} ion, while the latter peaks are from the intra-$4f^8$ transitions[45,46]. Under the excitation wavelength of 268 nm or 378 nm, the $NaBa_3La_3Si_6O_{20}$:0.20 Tb^{3+} sample emits green light with main peaks at 412, 435, 457, 488, 542, 581 and 622 nm, which can be ascribed to the $^5D_4$–^7F_J ($J = 6$, 5, 4 and 3) transitions of the Tb^{3+} ion. However, because the f–f absorption is a forbidden transition, only some narrow f–f transition lines locate in the excitation range of n-UV LED in spite of difficultly bumping the Tb^{3+} ion[47]. There is an overlap between the emission band (magenta line in Fig. 3(a)) of the Ce^{3+} ions and the f–f transition (olive line in Fig. 3(a)) absorption band of the Tb^{3+} ions, therefore, it is potential that the Ce^{3+} ions can be sensitizers to transfer energy to the Tb^{3+} ions to enhance their absorption. As shown in Fig. 3(b), the PL spectrum of the $NaBa_3La_3Si_6O_{20}$:Ce^{3+}, Tb^{3+} phosphors exhibits broad emission bands corresponding to the allowed f–d transition of the Ce^{3+} ions and the $^5D_4$–^7F_J characteristic transitions of

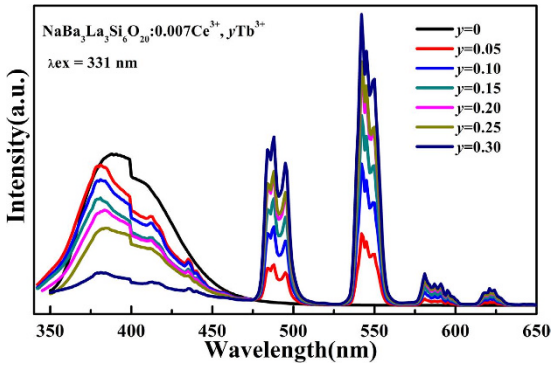

Figure 4. The PL spectra of the $NaBa_3La_3Si_6O_{20}$:0.007Ce^{3+}, yTb^{3+} phosphors.

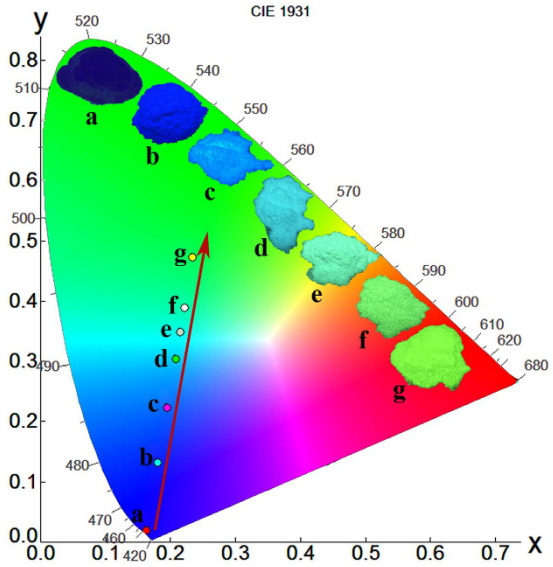

Figure 5. The CIE chromaticity coordinates of the $NaBa_3La_3Si_6O_{20}$:0.007Ce^{3+}, yTb^{3+} phosphors ($0 \leq y \leq 0.3$) excited under 331 nm and the pictures of the $NaBa_3La_3Si_6O_{20}$:0.007Ce^{3+}, yTb^{3+} phosphors ($0 \leq y \leq 0.3$) in a 365 nm UV box.

the Tb^{3+} ions. The emission intensity of the $NaBa_3La_3Si_6O_{20}$:Tb^{3+} samples under excitation wavelength of 268 nm is larger than that under 378 nm, because the intensity of the absorption peak centered at 268 nm is more intense than that at 378 nm. However, the emission light intensity monitored at 268 nm is less than that at 374 nm in the $NaBa_3La_3Si_6O_{20}$:Ce^{3+}, Tb^{3+} phosphors. These results verify that it is the overlap between *f-f* transition (peaking at 374 nm) but not *f-d* transition (peaking at 268 nm) of the Tb^{3+} ions and the emission band of the Ce^{3+} ions induce the energy transfer. Figure 3(b) also shows the excitation spectrum of the $NaBa_3La_3Si_6O_{20}$:0.007Ce^{3+}, 0.20Tb^{3+} phosphor monitored at 378 nm (the Ce^{3+} ions emission) is similar to that of at 542 nm (the Tb^{3+} ions emission) except the difference of luminous intensity, which provides another evidence for energy transfer of $Ce^{3+} \rightarrow Tb^{3+}$.

To further investigate the sensitized luminescence of the Tb^{3+} ions by the Ce^{3+} ions, the emission spectra of the $NaBa_3La_3Si_6O_{20}$:0.007Ce^{3+}, yTb^{3+} phosphors were measured (Fig. 4). Although the amount of the Ce^{3+} ions is fixed, their emission intensity gradually decreases along with the increase of the concentration of the Tb^{3+} ions. The result indicates that a lot of Tb^{3+} ions as acceptors accelerate energy diffusion of donors, which speeds up the average transfer rate of $Ce^{3+} \rightarrow Tb^{3+}$.

Figure 5 and Table 1 show the variation of Commission International deL'Eclairage (CIE) chromaticity coordinates of the $NaBa_3La_3Si_6O_{20}$:0.007Ce^{3+}, yTb^{3+} phosphors ($y = 0$, 0.05, 0.10, 0.15, 0.20, 0.25, 0.30) under excitation wavelength at 331 nm. The insets of Fig. 5 are the photographs of the $NaBa_3La_3Si_6O_{20}$:0.007Ce^{3+}, yTb^{3+} phosphors with different amount Tb^{3+} ions in a 365 nm *n*-UV lamp box. These results indicate that the emission light color can be modulated from deep blue to green only by varying the contention of the Tb^{3+} ions. Therefore the $NaBa_3La_3Si_6O_{20}$:Ce^{3+}, yTb^{3+} samples can be potential color-tunable phosphors for application in *n*-UV based WLED devices.

Energy transfer mechanism. In general, the energy transfer from a sensitizer to an activator in oxide may take place via exchange interaction or electric multipolar interaction[48]. The separation distance R_{Ce-Tb} can be also estimated from equation (1). Here, *x* is the total concentration of the Ce^{3+} and Tb^{3+} ions, where the

No. of points in CIE diagram	Sample compositions $NaBa_3La_3Si_6O_{20}$:0.007Ce^{3+}, yTb^{3+}	CIE coordinates (*x*, *y*)
a	y = 0.00	(0.163, 0.019)
b	y = 0.05	(0.181, 0.131)
c	y = 0.10	(0.195, 0.222)
d	y = 0.15	(0.208, 0.303)
e	y = 0.20	(0.216, 0.348)
f	y = 0.25	(0.223, 0.389)
g	y = 0.30	(0.235, 0.472)

Table 1. The comparison of the CIE chromaticity coordinates of the $NaBa_3La_3Si_6O_{20}$:0.007Ce^{3+}, yTb^{3+} phosphors (λ_{ex} = 331 nm).

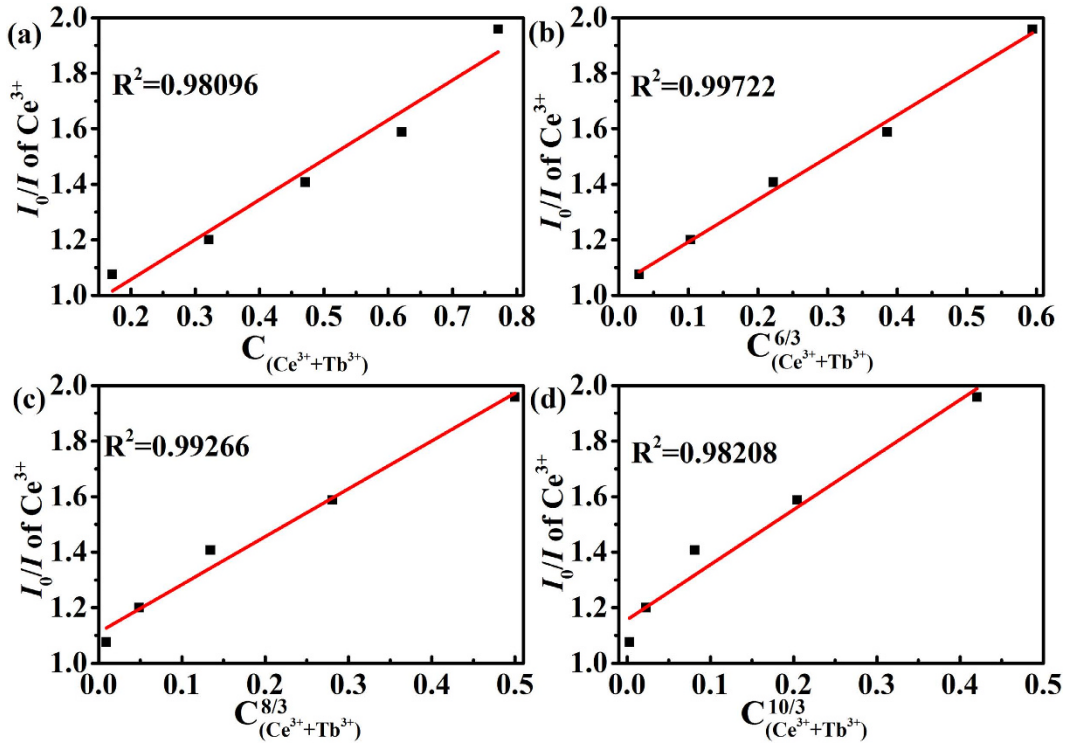

Figure 6. The dependence of I_0/I of the Ce^{3+} ions on (**a**) $C_{Ce^{3+}+Tb^{3+}}$ (**b**) $C^{6/3}_{Ce^{3+}+Tb^{3+}}$ (**c**) $C^{8/3}_{Ce^{3+}+Tb^{3+}}$ (**d**) $C^{10/3}_{Ce^{3+}+Tb^{3+}}$.

luminescence intensity of sensitizer is half of that in samples lack of activator. For the $NaBa_3La_3Si_6O_{20}$:Ce^{3+}, Tb^{3+} phosphors, the value of $x_{Ce^{3+}}$ and $x_{Tb^{3+}}$ is about 0.021 and 0.75 respectively, thus R_{Ce-Tb} is calculated to be about 7.5 Å. Since exchange interaction was restricted to distances of about 4 Å, the energy transfer mechanism of $Ce^{3+} \rightarrow Tb^{3+}$ should may be electric multipolar interaction[43,44].

According to Dexter's energy transfer expressions of multipolar interaction and Reisfeld's approximation, the following relation can be given as[42,48–51]:

$$\frac{\eta_0}{\eta} \propto C^{n/3}_{Ce^{3+}+Tb^{3+}} \tag{2}$$

where η_0 and η are the luminescence quantum efficiency of the Ce^{3+} ions in absence and presence of the Tb^{3+} ions, $n = 6$, 8 and 10 are corresponding to dipole – dipole, dipole – quadrupole and quadrupole – quadrupole interactions, respectively. The value η_0/η is approximately estimated by the ratio of related luminescence intensity I_0/I, I_0 is the intrinsic luminescence intensity of the Ce^{3+} ions, and I is the luminescence intensity of the Ce^{3+} ions in presence of the Tb^{3+} ions. Figure 6(a–d) illustrates the relationships between I_0/I and $C_{Ce^{3+}+Tb^{3+}}$ as well as I_0/I and $C^{n/3}_{Ce^{3+}+Tb^{3+}}$. The R^2 value is reasonable in Fig. 6(b,c), implying the energy transfer of $Ce^{3+} \rightarrow Tb^{3+}$ may occur via dipole–dipole or dipole–quadrupole interaction. However, Sommerdijk stated the probability of energy transfer of $Ce^{3+} \rightarrow Tb^{3+}$ via electric dipole-dipole interaction was less likely, therefore, dipole – quadrupole interaction should mainly contribute to energy transfer of $Ce^{3+} \rightarrow Tb^{3+}$ [52].

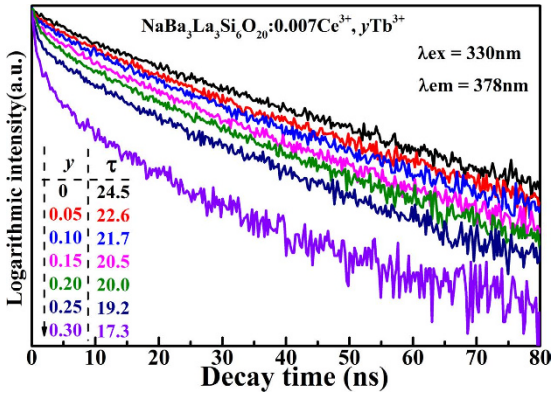

Figure 7. The decay curves for the emission of the Ce^{3+} ions in the $NaBa_3La_3Si_6O_{20}$:0.007Ce^{3+}, yTb^{3+} phosphors excited under 330 nm and monitored at 378 nm.

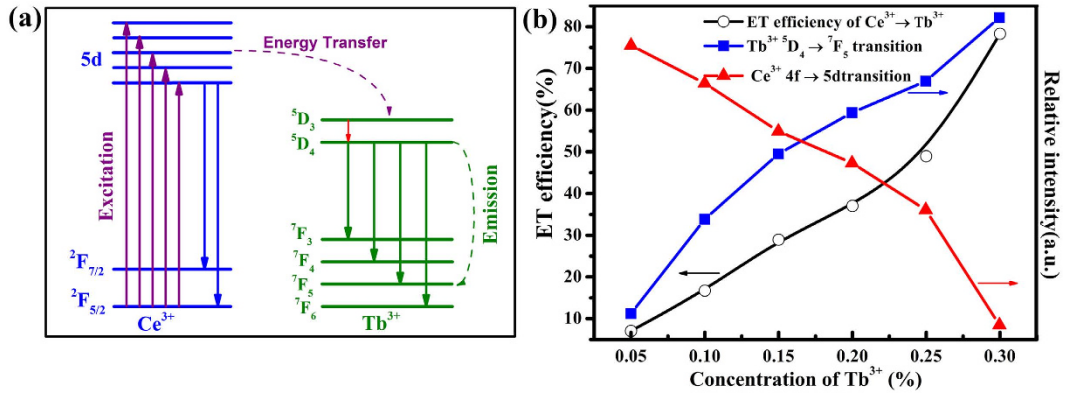

Figure 8. (**a**) The energy levels model for the energy transfer processes of $Ce^{3+} \rightarrow Tb^{3+}$. (**b**) The dependence of the emission of the Ce^{3+} ions and Tb^{3+} ions, and the energy transfer of $Ce^{3+} \rightarrow Tb^{3+}$ on the doping concentration of the Tb^{3+} ions in the $NaBa_3La_3Si_6O_{20}$:0.007Ce^{3+}, yTb^{3+} phosphors.

In order to further validate the energy transfer process, the room temperature decay curves for the 4*f*-5*d* (centered at 378 nm) transition of the Ce^{3+} ions in $NaBa_3La_3Si_6O_{20}$:0.007Ce^{3+}, yTb^{3+} ($y = 0.05$, 0.10, 0.15, 0.20, 0.25 and 0.30) excited at 330 nm are shown in Fig. 7 For existing two types of Ce^{3+} ions in topic phosphors, the decay curves should be well fitted with a typical two exponential function[53]:

$$I(t) = I_0 + A_1 \exp(-t/\tau_1) + A_2 \exp(-t/\tau_2) \quad (3)$$

where $I(t)$ and I_0 are the luminescence intensity at time t, A_1 and A_2 are the fitting constants, τ_1 and τ_2 represent the decay time for the exponential components. Then the average lifetime (τ^*) can be calculated to be 24.5, 22.6, 21.7, 20.5, 20.0, 19.2 and 17.3 by the following formula[40,54]:

$$\tau^* = \frac{A_1\tau_1^2 + A_2\tau_2^2}{A_1\tau_1 + A_2\tau_2} \quad (4)$$

The decay time of the Ce^{3+} ions decreases as increase of the concentration of the Tb^{3+} ions, which strongly demonstrates the energy transfer of $Ce^{3+} \rightarrow Tb^{3+}$.

Subsequently the energy levels model for the energy transfer processes of $Ce^{3+} \rightarrow Tb^{3+}$ was investigated. As given in Fig. 8(a), the Ce^{3+} ion absorbs light firstly, then it jumps from the ground states ($^2F_{5/2}$) to the excited states (5*d* energy levels), subsequently the excited state Ce^{3+} ion returns to the lowest level of 5d levels by giving off excess energy to its surroundings, eventually goes back to the $^2F_{7/2}$ or $^2F_{5/2}$ ground states by a radiative process. The energy transfer efficiency of $Ce^{3+} \rightarrow Tb^{3+}$ should increase as the increase of the concentration of the Tb^{3+} ions due to more neighboring Tb^{3+} ions around the Ce^{3+} ions. Finally the energy level transitions of $^5D_4$ to ^7F_J ($J = 3$, 4, 5 and 6) produce the characteristic emission of the Tb^{3+} ions.

The energy transfer efficiency η_T from the Ce^{3+} ions to the Tb^{3+} ions can be calculated according to the following equation[55]:

$$\eta_T = 1 - \frac{I_y}{I_0} \quad (5)$$

where I_0 and I_y are the emission light intensity of the sensitizer with and without an activator, respectively. In the $NaBa_3La_3Si_6O_{20}$:0.007Ce^{3+}, yTb^{3+} samples, the Ce^{3+} ion is a sensitizer and the Tb^{3+} ion is an activator. The η_T values can be calculated as 7.06%, 16.71%, 28.95%, 37.04%, 48.95%, 78.31%, as a function of y ($y = 0.15$, 0.30, 0.45, 0.60, 0.75, 0.90), respectively (Fig. 8(b)). The energy transfer of $Ce^{3+} \rightarrow Tb^{3+}$ is consistent with the conclusion that the energy transfer efficiency increases as the increase of the concentration of the Tb^{3+} ions due to more neighboring Tb^{3+} ions around the Ce^{3+} ions and is equivalent to that of the reported K_2MgSiO_4:Ce^{3+}, Tb^{3+} silicate phosphor[56].

Conclusion

A series of novel $NaBa_3La_3Si_6O_{20}$:Ce^{3+}, Tb^{3+} phosphors were prepared by solid state method. The energy transfer processe of $Ce^{3+} \rightarrow Tb^{3+}$ has been demonstrated to be dipole – quadrupole interaction. The tunable colors from deep blue to green can be realized by varying the doping concentration of the Tb^{3+} ions under the irradiation of 331 nm. These results demonstrate the as-prepared $NaBa_3La_3Si_6O_{20}$:Ce^{3+}, Tb^{3+} samples can act as potential *n*-UV based w-LED phosphors.

Experimental Section. *Compounds synthesis.* The $NaBa_3La_3Si_6O_{20}$:Ce^{3+}, Tb^{3+} phosphors were synthesized by high temperature solid state method. Na_2CO_3 (A.R.), $BaCO_3$ (A.R.), SiO_2 (A.R.), La_2O_3 (99.99%), CeO_2 (99.99%) and Tb_4O_7 (99.99%) were purchased from Sinopharm Chemical Reagent Co., Ltd. All of the initial chemicals were used without further purification. Stoichiometric amounts of the above-mentioned chemicals were ground thoroughly by an agate mortar, packed tightly in an alumina crucible. The temperature of the furnace was heated up to 500 °C at a rate of 60 °C/h, then held for 24 h to preheat the mixture in air atmosphere. After the mixture was ground once again, the temperature was increased to 930 °C at a rate of 60 °C/h and held for 100 h with four intermittent grindings. Finally, the prepared phosphors were cooled to room temperature and reground into resulting phosphors. For convenient expression, $NaBa_3La_{3-3x-3y}Ce_{3x}Tb_{3y}Si_6O_{20}$ is abbreviated as $NaBa_3La_3Si_6O_{20}$:$x$$Ce^{3+}$, $y$$Tb^{3+}$. For example, $NaBa_3La_{2.55}Ce_{0.15}Tb_{0.30}Si_6O_{20}$ is denoted as $NaBa_3La_3Si_6O_{20}$:0.05Ce^{3+}, 0.10Tb^{3+}.

Material characterization. The powder XRD measurements were taken on a Bruker D8 X-ray diffractometer with a Cu Kα source ($\lambda = 1.5418$ Å) in the angular range from 5° to 80° with a scanning step of 0.15. The structure refinement was carried out with the General Structure Analysis (GSAS) and EXPGUI software[57,58]. XRD Rietveld profile refinements of the structural models were performed using the General Structure Analysis (GSAS) software. The photoluminescence (PL) and photoluminescence excitation (PLE) spectra were obtained by an FLS-980 fluorescence spectrophotometer equipped with a 450 W Xe light source. The photoluminescence lifetime curves were measured on an FLS-920 fluorescence spectrophotometer equipped with a laser as light source. All measurements were performed at room temperature. The element analyses of samples were performed by the (X-ray fluorescence) XRF method on a thermo ARL ADVANTXP+ apparatus.

References

1. Schubert, E. F. & Kim, J. K. Solid-state light sources getting smart. *Science* **308,** 1274–1278 (2005).
2. Shur, M. S. & Zukauskas, R. Solid-state lighting: toward superior illumination. *P. Ieee*. **93,** 1691–1703 (2005).
3. Narukawa, Y. *et al.* Recent progress of high efficiency white LEDs. *Phys. Status. Solidi. A* **204** (2007).
4. Tsao, J. Y., Coltrin, M. E., Crawford, M. H. & Simmons, J. A. Solid-state lighting: an integrated human factors, technology, and economic perspective. *P. Ieee*. **98,** 1162–1179 (2010).
5. Bando, K., Sakano, K., Noguchi, Y. & Shimizu, Y. Development of high-bright and pure-white LED Lamps. *J. Illum. Eng. Soc.* **22,** 1–5 (1998).
6. Hye Oh, J., Ji Yang, S. & Rag Do, Y. Healthy, natural, efficient and tunable lighting: four-package white LEDs for optimizing the circadian effect, color quality and vision performance. *Light-Sci. Appl.* **3,** e141 (2014).
7. Setlur, A. A., Heward, W. J., Hannah, M. E. & Happek, U. Incorporation of Si^{4+}–N^{3-} into Ce^{3+}-Doped Garnets for Warm White LED Phosphors. *Chem. Mater.* **20,** 6277–6283 (2008).
8. Setlur, A. A. *et al.* Crystal chemistry and luminescence of Ce^{3+}-doped $Lu_2CaMg_2(Si,Ge)_3O_{12}$ and its use in LED based lighting. *Chem. Mater.* **18,** 3314–3322 (2006).
9. Lü, W. *et al.* A novel efficient Mn^{4+} activated $Ca_{14}Al_{10}Zn_6O_{35}$ phosphor: application in red-emitting and white LEDs. *Inorg. Chem.* **53,** 11985–11990 (2014).
10. Wang, L. *et al.* Enriching red emission of $Y_3Al_5O_{12}$:Ce^{3+} by codoping Pr^{3+} and Cr^{3+} for improving color rendering of white LEDs. *Opt. Express*. **18,** 25177–25182 (2010).
11. Lee, S.-P., Huang, C.-H., Chan, T.-S. & Chen, T.-M. New Ce^{3+}-activated thiosilicate phosphor for LED lighting—synthesis, luminescence studies, and applications. *ACS Appl. Mat. Inter.* **6,** 7260–7267 (2014).
12. Hao, Z. *et al.* White light emitting diode by using α-$Ca_2P_2O_7$:Eu^{2+}, Mn^{2+} phosphor. *Appl. Phys. Lett.* **90,** 261113 (2007).
13. Yang, W.-J. & Chen, T.-M. Ce^{3+}/Eu^{2+} codoped Ba_2ZnS_3: A blue radiation-converting phosphor for white light-emitting diodes. *Appl. Phys. Lett.* **90,** 171908 (2007).
14. Kim, J. S. *et al.* White-light generation through ultraviolet-emitting diode and white-emitting phosphor. *Appl. Phys. Lett.* **85,** 3696–3698 (2004).
15. Piao, X., Horikawa, T., Hanzawa, H. & Machida, K.-i. Characterization and luminescence properties of $Sr_2Si_5N_8$:Eu^{2+} phosphor for white light-emitting-diode illumination. *Appl. Phys. Lett.* **88,** 161908 (2006).
16. Lee, S. H., Park, J. H., Son, S. M., Kim, J. S. & Park, H. L. White-light-emitting phosphor: $CaMgSi_2O_6$:Eu^{2+}, Mn^{2+} and its related properties with blending. *Appl. Phys. Lett.* **89,** 221916 (2006).
17. Xia, Z. G. *et al.* Chemical unit cosubstitution and tuning of photoluminescence in the $Ca_2(Al_{1-x}Mg_x)(Al_{1-x}Si_{1+x})O_7$:$Eu^{2+}$ phosphor. *J. Am. Chem. Soc.* **137,** 12494–12497 (2015).
18. Bai, G., Tsang, M.-K. & Hao, J. Tuning the luminescence of phosphors: beyond conventional chemical method. *Adv. Opt. Mater.* **3,** 431–462 (2015).
19. Xia, Z. & Liu, R.-S. Tunable blue-green color emission and energy transfer of $Ca_2Al_3O_6F$:Ce^{3+},Tb^{3+} phosphors for near-UV white LEDs. *J. Phys. Chem. C* **116** (2012).
20. Zhang, X., Zhou, L., Pang, Q., Shi, J. & Gong, M. Tunable luminescence and $Ce^{3+} \rightarrow Tb^{3+} \rightarrow Eu^{3+}$ energy transfer of broadband-excited and narrow line red emitting Y_2SiO_5:Ce^{3+}, Tb^{3+}, Eu^{3+} phosphor. *J. Phys. Chem. C* **118,** 7591–7598 (2014).

21. Xia, Z. G. *et al.* Tuning of photoluminescence by cation nanosegregation in the $(CaMg)_x(NaSc)_{1-x}Si_2O_6$ solid solution. *J. Am. Chem. Soc.* **138,** 1158–1161 (2016).
22. Kang, F. *et al.* Red photoluminescence from Bi^{3+} and the influence of the oxygen-vacancy perturbation in $ScVO_4$: a combined experimental and theoretical study. *J. Phys. Chem. C* **118,** 7515–7522 (2014).
23. Kang, F., Peng, M., Zhang, Q. & Qiu, J. Abnormal anti-quenching and controllable multi-transitions of Bi^{3+} luminescence by temperature in a yellow-emitting $LuVO_4$:Bi^{3+} phosphor for UV-Converted white LEDs. *Chem–Eur J.* **20,** 11522–11530 (2014).
24. Peng, M. & Wondraczek, L. Bi^{2+}-doped strontium borates for white-light-emitting diodes. *Opt. Lett.* **34,** 2885–2887 (2009).
25. Guo, C., Luan, L., Xu, Y., Gao, F. & Liang, L. White light–generation phosphor $Ba_2Ca(BO_3)_2$:Ce^{3+}, Mn^{2+} for light-emitting diodes. *J. Electrochem. Soc.* **155,** J310–J314 (2008).
26. Su, Y., Li, L. & Li, G. Synthesis and optimum luminescence of $CaWO_4$-based red phosphors with codoping of Eu^{3+} and Na^+. *Chem. Mater.* **20,** 6060–6067 (2008).
27. Yan, S. *et al.* Enhanced red emission in $CaMoO_4$:Bi^{3+}, Eu^{3+}. *J. Phys. Chem. C* **111,** 13256–13260 (2007).
28. Pust, P. *et al.* Narrow-band red-emitting $Sr[LiAl_3N_4]$:Eu^{2+} as a next-generation LED-phosphor material. *Nat. Mater.* **13,** 891–896 (2014).
29. Xia, Z. G., Miao, S. H., Molokeev, M. S., Chen, M. Y. & Liu, Q. L. Structure and luminescence properties of Eu^{2+} doped $Lu_xSr_{2-x}SiN_xO_{4-x}$ phosphors evolved from chemical unit cosubstitution. *J. Mater. Chem. C* **4,** 1336–1344 (2016).
30. Liu, X. *et al.* Single-phased white-emitting $12CaO{\cdot}7Al_2O_3$:Ce^{3+}, Dy^{3+} phosphors with suitable electrical conductivity for field emission displays. *J. Mater. Chem.* **22,** 16839–16843 (2012).
31. Lü, W. *et al.* Tunable color of Ce^{3+}/Tb^{3+}/Mn^{2+}-coactivated $CaScAlSiO_6$ via energy transfer: a single-component red/white-emitting phosphor. *Inorg. Chem.* **52,** 3007–3012 (2013).
32. Lü, W. *et al.* Tunable full-color emitting $BaMg_2Al_6Si_9O_{30}$:Eu^{2+},Tb^{3+},Mn^{2+} phosphors based on energy transfer. *Inorg. Chem.* **50,** 7846–7851 (2011).
33. Opstelte, J. j., Radielov, D. & Wanmaker, W. L. Choice and evaluation of phosphors for application to lamps with improved color rendition. *J. Electrochem. Soc.* **120,** 1400–1408 (1973).
34. Nag, A. & Kutty, T. R. N. Photoluminescence due to efficient energy transfer from Ce^{3+} to Tb^{3+} and Mn^{2+} in (Sr_3AlSiO_{20})-Si-10. *Mater. Chem. Phys.* **91,** 524–531 (2005).
35. Heyward, C. C., McMillen, C. D. & Kolis, J. W. Hydrothermal growth of lanthanide borosilicates: a useful approach to new acentric crystals including a derivative of cappelenite. *Inorg. Chem.* **54** (2015).
36. Sanjeewa, L. D. *et al.* Hydrothermal synthesis, structure, and property characterization of rare earth silicate compounds: $NaBa_3Ln_3Si_6O_{20}$ (Ln = Y, Nd, Sm, Eu, Gd). *Solid. State. Sci.* **48,** 256–262 (2015).
37. Shannon, R. D. & Prewitt, C. T. Effective Ionic radii in oxides and fluorides. *Acta. Crystallogr. B* **25,** 925 (1969).
38. Dorenbos, P. The 5d level positions of the trivalent lanthanides in inorganic compounds. *J. Lumin.* **91,** 155–176 (2000).
39. Park, H. K., Oh, J. H., Kang, H., Zhang, J. & Do, Y. R. Hybrid 2D photonic crystal-assisted $Lu_3Al_5O_{12}$:Ce ceramic-plate phosphor and free-standing red film phosphor for white LEDs with high color-rendering index. *ACS Appl. Mat. Inter.* **7,** 4549–4559 (2015).
40. Shang, M. *et al.* Blue emitting $Ca_8La_2(PO_4)_6O_2$:Ce^{3+}/Eu^{2+} phosphors with high color purity and brightness for white LED: soft-chemical synthesis, luminescence, and energy transfer properties. *J. Phys. Chem. C* **116,** 10222–10231 (2012).
41. Lian, Z. *et al.* Crystal structure refinement and luminescence properties of Ce^{3+} singly doped and Ce^{3+}/Mn^{2+} co-doped $KBaY(BO_3)_2$ for n-UV pumped white-light-emitting diodes. *RSC Adv.* **3,** 16534–16541 (2013).
42. Dexter, D. L. & Schulman, J. H. Theory of concentration quenching in inorganic phosphors. *J. Chem. Phys.* **22,** 1063–1070 (1954).
43. Blasse, G. Energy transfer in oxidic phosphors. *Philips. Res. Rep.* **24,** 131 (1969).
44. Dexter, D. L. A theory of sensitized luminescence in solids. *J. Chem. Phys.* **21,** 836–850 (1953).
45. Bourcet, J. C. & Fong, F. K. Quantum efficiency of diffusion limited energy-transfer in $La_{1-X-Y}Ce_xTb_yPO_4$. *J. Chem. Phys.* **60,** 34–39 (1974).
46. Liang, C. *et al.* A novel tunable blue-green-emitting $CaGdGaAl_2O_7$:Ce^{3+}, Tb^{3+} phosphor via energy transfer for UV-excited white LEDs. *Dalton Trans.* **44,** 8100–8106 (2015).
47. Ryan, J. L. & Jorgense, C. k. Absorption spectra of octahedral lanthanide hexahalides. *J. Phys. Chem.* **70,** 2845 (1966).
48. Reisfeld, R., Greenber, E., Velapold, R. & Barnett, B. Luminescence quantum efficiency of Gd and Tb in borate glasses and mechanism of energy-transfer between them. *J. Chem. Phys.* **56,** 1698 (1972).
49. Lahoz, F., Martin, I. R., Mendez-Ramos, J. & Nunez, P. Dopant distribution in a Tm^{3+}-Yb^{3+} codoped silica based glass ceramic: an infrared-laser induced upconversion study. *J. Chem. Phys.* **120,** 6180–6190 (2004).
50. Huang, C. H. & Chen, T. M. A novel single-composition trichromatic white-light $Ca_3Y(GaO)_3(BO_3)_4$:Ce^{3+}, Mn^{2+}, Tb^{3+} phosphor for UV-Light emitting diodes. *J. Phys. Chem. C* **115,** 2349–2355 (2011).
51. Jia, Y. C., Qiao, H., Zheng, Y. H., Guo, N. & You, H. P. Synthesis and photoluminescence properties of Ce^{3+} and Eu^{2+}-activated $Ca_7Mg(SiO_4)_4$ phosphors for solid state lighting. *Phys. Chem. Chem. Phys.* **14,** 3537–3542 (2012).
52. Verstegen, J. M. P. J., Sommerdijk, J. L. & Verriet, J. G. Cerium and terbium luminescence in $LaMgAl_{11}O_{19}$. *J. Lumin.* **6,** 425–431 (1973).
53. Lephoto, M. A. *et al.* Synthesis and characterization of $BaAl_2O_4$:Eu^{2+} co-doped with different rare earth ions. *Physica. B* **407,** 1603–1606 (2012).
54. Zhu, G. *et al.* $Ca_5La_5(SiO_4)_3(PO_4)_3O_2$:$Ce^{3+}$, Mn^{2+}: A color-tunable phosphor with efficient energy transfer for white-light-emitting diodes. *J. Electrochem. Soc.* **158,** J236–J242 (2011).
55. Paulose, P. I., Jose, G., Thomas, V., Unnikrishnan, N. V. & Warrier, M. K. R. Sensitized fluorescence of Ce^{3+}/Mn^{2+} system in phosphate glass. *J. Phys. Chem. Solids* **64,** 841–846 (2003).
56. Xia, Y. F. *et al.* Luminescence properties and energy transfer in K_2MgSi_4:Ce^{3+}, Tb^{3+} as a green phosphor. *Mater. Express.* **6,** 37–44 (2016).
57. Larson, A. C. & Dreele, R. B. von *GASA, General Structure Analysis System*. (LANSCE, MS-H805). *Los Alamos National Laboratory Los Alaoms, NM* (1994).
58. Toby, B. H. EXPGUI, a graphical user interface for GSAS. *J. Appl. Crystallogr.* **34,** 210–213 (2001).

Acknowledgements

We acknowledge the financial support from the National Natural Science Foundation of China (Grant No. 51502307) and Key Laboratory of Coordination Chemistry and Functional Materials in Universities of Shandong, Dezhou University.

Author Contributions

M.X. developed the idea and supervised the project, Z.J. and M.X. conducted the experiments and wrote the paper. All authors discussed the results.

Additional Information

Supplementary information accompanies this paper at http://www.nature.com/srep

Competing financial interests: The authors declare no competing financial interests.

How to cite this article: Jia, Z. and Xia, M. Blue-green tunable color of Ce^{3+}/Tb^{3+} coactivated $NaBa_3La_3Si_6O_{20}$ phosphor via energy transfer. *Sci. Rep.* **6**, 33283; doi: 10.1038/srep33283 (2016).


This work is licensed under a Creative Commons Attribution 4.0 International License. The images or other third party material in this article are included in the article's Creative Commons license, unless indicated otherwise in the credit line; if the material is not included under the Creative Commons license, users will need to obtain permission from the license holder to reproduce the material. To view a copy of this license, visit http://creativecommons.org/licenses/by/4.0/

© The Author(s) 2016